Bulgarian Chemical Communications, Volume 52, Issue (pp. 525-531) 2020 *DOI: 10.34049/bcc.52.4.MP04*

Organic solvent nanofiltration of extracts from *Hypericum Perforatum L.*: effect of variable feed composition on rejection and flux decline

I. Saykova[1]*, I. Trayanov[1,2] M. Bojkova[1], N. Stoilova[3], M. Funeva-Peycheva[3]

[1]*Department of Chemical Engineering, Faculty of Chemical and System Engineering, University of Chemical Technology and Metallurgy, Sofia, Bulgaria*
[2]*Institute of Chemical Engineering, Bulgarian Academy of Sciences, Sofia, Bulgaria*
[3]*Central Laboratory for Veterinary-Sanitary Expertise and Ecology, Sofia, Bulgaria*

Received October 3, 2020; Revised November 11, 2020

The medicinal plant *Hipericum Perforatum* is traditionally used as a herbal remedy and food supplement because of its versatile bioactive properties, in particular the anxiolytic and antidepressant activities. The extraction and separation of the specific active compounds hypericins is still problematic because of their very low and variable content (standardized to 0.3% in the extract), poor solubility in water, and extreme sensitivity to light, pH, and heat. In this context, this work evaluates the potentiality of using a direct nanofiltration process to promote the enrichment of extracts in hypericins relatively to other largely present compounds as polyphenol and flavonoids. By using ethanolic extracts obtained by different methods and different raw materials, the effect of variation in feed composition on permeate flux, concentration and content of effective components were investigated in dead-end mode at a fixed pressure (5-20 bar) and stirring speed (350 rpm). The set of the four commercial flat-sheet membranes (DuraMem™ 200, 500, and 900 and StarMem™240) displayed very distinct permeation patterns in terms of rejections and fluxes. Hermia's fouling models were considered to explain the flux decline and fouling phenomena during concentration of extracts. According to the experiments, the membrane with a larger pore size (900 Da) had the highest average flux of 26.5 $Lm^{-2}h^{-1}$ and a higher propensity to fouling. The membrane with a lower cut-off (200 Da) having rejections above 95%, could be selected for concentration of the extracts, but also some other high-value small molecules, such as gamma aminobutyric acid (GABA) identified and quantified, using HPLC/MS, can be simultaneously recovered only in the permeate stream with 200 Da membrane.

Keywords: nanofiltration, *Hipericum Perforatum*, extract enrichment

INTRODUCTION

Considering the increased recognition of health benefits of plant extracts and their utilization in the food, pharmaceutical and cosmetic industries, it is of interest investigating into efficient and cost-effective separation processes for better control of the properties of the final products [1]. Nowadays, membrane-based technologies, e.g. microfiltration (MF), ultrafiltration (UF), nanofiltration (NF), membrane distillation, and pervaporation, have demonstrated meeting the requirements and are involved in different food and byproduct processes owing to the technology's advantages as high selectivity, mild processing conditions, and low energy consumption over other (in many cases thermally driven) separation processes. Polymer membranes, as well the newer class of organic solvent-resistant NF membranes (100-1000 Da) and tight UF membranes (1-3 kDa) and their combinations have been recognized for their capability to recover valuable compounds from various natural and processed products [2-4]. Several successful OSN applications have been reported for increasing the concentration of dilute species from lower molecular-weight solvents, and providing recycling of organic solvents, recovery of aromas, fractionation of bioactive compounds as phenolic compounds and other antioxidants, as the most popular ones.

Fouling represents a real limitation in any membrane separation, but for NF it might be even more complex because of the interactions between membrane-solvent-solutes taking place at nanoscale and being difficult to understand and to predict [5]. Membrane fouling is a complex multi-scale (occurring both on the membrane surface and in the membrane pores) and multi-physical phenomenon depending on many inter-related factors, including the operating conditions, membrane properties and feed characteristics. Membrane fouling formed during treatment of plant extracts could be especially prevalent as often more than 80% of the components present in the extracts are non-active macromolecules that can easily block the membrane pores. Regarding the therapeutic effect, typically the whole herbal extracts are considered as active compounds because of the synergy among the various secondary and primary metabolites, so their

* To whom all correspondence should be sent:
E-mail: i.seikova@uctm.edu

preservation and as minor as possible change in their properties during processing is very important.

The objectives of this work are to evaluate the combination of extraction followed by Organic Solvent Nanofiltration (OSN) for the concentration of ethanolic (96%) extracts from *Hypericum perforatum* and to provide a prediction of the fouling mechanisms responsible for the flux decline involved in dead-end mode.

EXPERIMENTAL

Solvent extraction and analysis

The plant extracts were prepared by using commercial samples of fractionated and non-fractionated dry material. Batch solid-liquid extraction was carried out at room temperature 20±2°C, liquid-to-solid ratio of 10 ml liquid/g solid, for 120 min under shaking, using 96% ethanol as solvent. Three different extracts were prepared, using the fraction of 1.25 mm (E1), non-fractionated material (E2), and the fraction of 0.9 mm (E3). To quantify the content of extractable compounds present in the plant, the extraction was carried out repeatedly with fresh solvent, until there were no significant differences from additional extractions (minimum 3 steps). The extracts were filtered through 0.2 μm PVDF syringe filters for removing suspended solids.

Plant extracts and OSN products (retantate, permeate, washing solutions) were characterized using standard spectrometric procedures with subsequent confirmation by HPLC/MS identification and quantification of some key components. The total hypericins content (THC) was measured by direct UV-Vis analysis at 590 nm. The total phenolic content (TPC) was determined colorimetrically according to the Folin-Ciocalteu method, and expressed as mg gallic acid equivalent (mg GAE g^{-1} plant material). The content of flavonoids was determined by the aluminium chloride method and expressed as mg quercetin equivalent (mg QE g^{-1}). The total solids content (TSC) was obtained by drying in an oven at 70 ± 1°C until constant weight.

Dead-end filtration experiments

Nanofiltration trials were carried out in a stirred dead-end cell (METCell, Membrane Extraction Technology, UK) with an effective membrane area of 54 cm². The cell was operated at a constant transmembrane pressure (TMP) up to 40 bar, regulated with high purity nitrogen gas, and stirred at 350 rpm by a magnetic stirrer plate. Four flat sheet OSN membranes from Evonik MET Ltd. with different molecular weight cut-off (MWCO), made of different materials, were used in this study (Table 1).

Table 1. OSN membranes employed and their characteristics (manufacturer's data)[b]

Membrane	M_w g mol^{-1}	Membrane type and material	Pressure bar	Nature	δ_{HSP}[c] $MPa^{1/2}$
StarMem™ 240	400[a]	Polyimide-based top layer (pore size <5 nm)	20	Hydrophobic	23.2
DuraMem™ series	200[b]	Crosslinked polyamide	20	Amphiphilic	26.8
	500[b]		20		
	900[b]		5-10		

[a] based on rejection of n-alkanes in toluene; [b] based on rejection of styrene oligomers in acetone; [c] total Hansen solubility parameter

The membrane conditioning was performed following the guidelines provided by the suppliers [5]. After filtration, the membrane was rinsed with ethanol, and the pure solvent was permeated at the operating pressure. All filtration experiments were conducted at room temperature, using a volume reduction factor (VRF) up to 6. The permeate volume was recorded at regular time intervals, and the volumetric flux was calculated according to:

$$J_v = \frac{1}{A}\frac{dV_p}{dt} \quad (1)$$

where V_p is the volume of permeate (L) collected in a certain time t (h) through the membrane filtration area A (m^2). The evolution of flux *vs* time was fitted by polynomial equation of second or third order and the average permeate flux was calculated by integration of J(t) function:

$$< J >= \frac{1}{t_n}\int_{t_1}^{t_n} J(t)dt \quad (2)$$

The observed rejection values (R_i) for a specific component group were defined as:

$$R_i(\%) = \left(1 - \frac{C_{p,i}}{C_{f,i}}\right)\cdot 100 \quad (3)$$

where $C_{f,i}$ and $C_{p,i}$ denote the feed and permeate (averaged over the time) concentration.

Fouling modeling

The mathematical analysis of the permeate flux behavior was performed based on Hermia's model that is a common approach employed in microfiltration, ultrafiltration and reverse osmosis to nanofiltration systems as well [7, 8]. The governing equation associates the "rate of blocking" of the membrane (d^2t/dV^2) with the instantaneous resistance (reciprocal of the flux rate dt/dV):

$$\frac{d^2t}{dV^2} = K\left(\frac{dt}{dV}\right)^n \quad (4)$$

where K is a rate constant and n is the blocking index equal to 2, 1.5, 1 or 0 for complete pore blocking, standard pore blocking, intermediate pore blocking and cake filtration, respectively.

On the basis of many studies on membrane fouling, it was determined that these mechanisms may occur individually or in some cases the relative importance of individual mechanisms can change with time. Many researchers have derived combined models such as the cake-complete blocking, cake-intermediate blocking, cake-standard blocking, and others, for the more complete coverage of fouling stages and the more realistic handling of complex fouling caused by multiple foulants [9, 10].

Table 2. Blocking models during constant-pressure dead-end operation

Model	V/A=f(t)	Physical concept
Cake layer formation (CLM)	$\frac{V}{A} = \frac{1}{K_{CL}J_0}\sqrt{1+2K_{CL}J_0^2 t} - 1)$	$d_{solute} >> d_{pore}$
Intermediate blocking (IBM)	$\frac{V}{A} = \frac{J_0}{K_{IB}}\ln(1+K_{IB}\cdot t)$	$d_{solute} \approx d_{pore}$
Standard blocking (SBM)	$\frac{V}{A} = t(\frac{K_{SB}}{2} + \frac{1}{J_0})^{-1}$	$d_{solute} << d_{pore}$
Complete blocking (CBM)	$\frac{V}{A} = \frac{J_0}{K_{CB}}(1-\exp^{-K_{CB}\cdot t})$	$d_{solute} \approx d_{pore}$
Complete blocking - Cake layer (Combined)	$\frac{V}{A} = \frac{J_0}{K_B}(1-\exp(\frac{-K_B}{K_C J_0^2}\sqrt{1+2K_c J_0^2 t} - 1)))$	Loss of active area plus rise in cake resistance

Table 2 presents the analytical expressions for the kinetic models used. More precisely, the relation between the cumulative permeate volume per unit area (V/A) and the filtration time (t) is considered, where J_0 is the initial permeate flux and K is the constant with the subscript indicating the blocking mechanism.

RESULTS AND DISCUSSION

Membrane selection

Hypericum perforatum is one of the most widely used and researched medicinal plants, and to date, at least 900 molecules with unique structure have been isolated and characterized [11]. Most relevant for the pharmacological activity are the characteristic naphthodianthrone pigments (hypericin, pseudohypericin) and the phloroglucinols (hyperforin, adhyperforin), along with the more common flavonoids, as glycosides of quercetin-like hyperoside, rutin, isoquercitrin, quercitrin, various flavonols; phenolic acids, oligomeric procyanidins, and tannins, among others.

The choice of a suitable membrane is mainly governed by the MWCO characteristics of the membranes, taking into account the size of the organic molecules relative to the membrane pore size, and the intended use. It is well accepted that the value of nominal MWCO provided by the manufacturer is an initial indication of the membrane operating range since it is dependent on the solvent-solute system used for testing. For polymeric membranes, the solvent used can interact with the membrane, resulting in compaction, solvation and differential swelling with enough impact to significantly alter separation/ fractionation properties in some systems [5].

Table 3 gives the range of variation of several physico-chemical properties of secondary metabolites of the plant affecting the transport across the membrane. In order to better account for the molecular size instead of its weight, the Stokes diameter (d_s) and diffusion coefficients (D_0) were calculated by using the Stokes-Einstein equation. Hansen solubility parameters (δ_{HSP}), including dispersion, polar and hydrogen bonding forces, that have proved to be a good first estimate for selecting membrane materials for specific organic-organic separations, were also calculated using group contribution methods [12].

Table 3. Physicochemical characteristics of the main constituents of *Hypericum perforatum*

Chemical class	Molar mass $gmol^{-1}$	d_s nm	D_0 $10^{-9}\ m^2s^{-1}$	Nature	δ_{HSP} $MPa^{1/2}$
Hypericins	504-522	0.9-1.0	2.2-2.1	Amphiphilic	42-42.8
Flavonoids	286-610	0.7-1.1	2.8-2.0	Lipophilic/hydrophilic	34-35.3
Phenolic acids	200- 578	0.6-1.0	3.3-2.1	Hydrophilic	17-32.6
Procyanidins	500-3000	0.9-2.2	2.2-1.1	Hydrophilic	25-33.2
Ethanol			1.58	Protic-polar	26.5

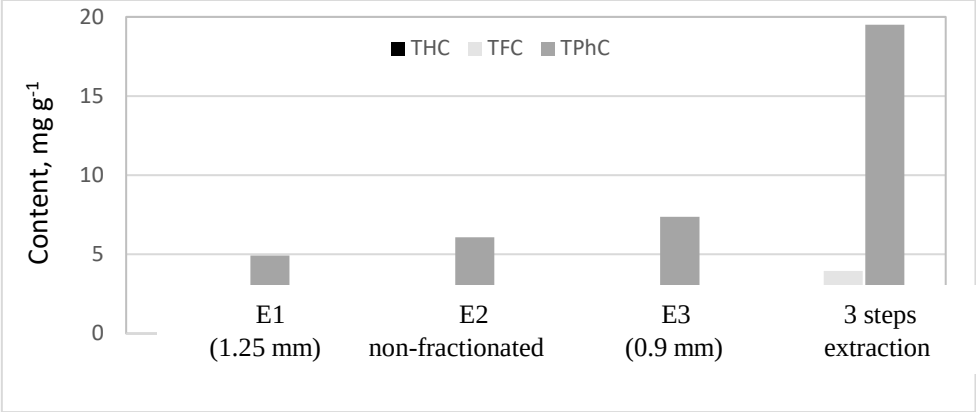

Figure 1. Contents of total hypericins (THC), flavonoids (TFC) and phenolics (TPC) in the feed extracts

Because of a broad size distribution (as seen in most natural extracts), *Hypericum perforatum* has both small molecules with high diffusivities and bigger molecules with low diffusivities. Most of the secondary metabolites, however, are low- to moderate-size species that correspond to an equivalent of Stokes diameter up to 1 nm. OSN membranes can reject molecules within the range 100-1000 Da, a reason why they could be used in concentrating natural extracts obtained with organic solvents. Given the reported amphiphilic character of DuraMem™ series (δ_{HSP}=26.8 $MPa^{1/2}$) and hydrophobic for StarMem™240 (δ_{HSP}=26.8 $MPa^{1/2}$), some specific interactions with the solvents and solutes would be expected [5, 6]. Taking these points into account, several OSN membranes were tested, covering almost the whole NF range, and the choice of membrane was based on the requirement of high rejection and minimum losses in the permeate for the key secondary metabolites.

Membrane performance under different process conditions

The content of classes of substances obtained by different extraction procedures, both one-step and sequential, are given in Fig. 1. They present high levels of polyphenols (up to 7.37 mg $GAEg^{-1}$), less amounts of flavonoids (up to 1.47 mg QE g^{-1}) and comparatively very low contents of hypericins (up to 0.15 mg $HYPg^{-1}$). In spite of using 96% ethanol instead of ethanol-water mixtures and low temperature of 20°C, yet significant TSC were obtained, varying between 0.05 and 0.1 g g^{-1}. The extraction yields after the single extraction were only 20-30% of the exhaustive 3-step extraction values used as a reference. The extraction from the fraction with low particle size (E3) allowed more complete recovery of all soluble compounds but the relative proportions of the minor THC and TFC in relation to the to TPC and TSC decreased.

A summary of the average permeate fluxes and rejections for the key compounds and total soluble solids is presented in Table 4. The values of pure solvent flux before ($J_{s,in}$) and after the extract filtration ($J_{s,f}$) are also presented.

Results demonstrate considerable variations in permeability, extending up to a factor over 45 for pure solvent (0.55 - 24.8 $Lm^{-2}bar^{-1}h^{-1}$) and 2-3 for feed extracts (0.11-0.96 $Lm^{-2}bar^{-1}h^{-1}$). No recovery of ethanol permeability was obtained after the physical cleaning performed, for all membranes. The rejection of particular fractions was revealed to depend on the used membrane and feed characteristics to much lower extent, all membranes having rejections of at least 80%, in addition to a high pigment retention capacity. These results are consistent with those of several studies that also reported retention from > 85 up to 100% for the concentration of phenolic compounds from the hydroethanolic extracts with the same membranes providing permeate fluxes in the same low range [1-4].

Table 4. Permeate fluxes and rejection values during OSN

Membrane	Extract	Fluxes, $L.m^{-2}h^{-1}$			Rejection, %			
		$J_{s,in}$	$< J >$	$J_{s,f}$	TSC	THC	TPC	TFC
DuraMem™900	E2	124.1	4.8	3.3	86.3	> 99	86.5	89.4
DuraMem™500	E1	11.2	4.4	4.3	94.3	> 99	91.2	93.9
	E2		2.4	3.5	95.1	> 99	94.1	97.7
	E3		1.7	2.1	91.2	> 99	95.3	93.1
StarMem™240	E1	30.1	6.5	8.1	86.1	> 99	84.4	90.8
	E2		4.9	6.3	85.2	> 99	83.3	84.9
DuraMem™200	E1	11	6.5	8.4	96.7	> 99	97.9	98.1

Nevertheless, the membrane with apparent cut-off of 900 Da has distinguished itself by providing a very high ethanol flux and permeating more solutes. That is, the retentions varied between 86% and 100%, more than 10% of TSC being found in the permeate. The membrane StarMem™240, also showing a large flux decline, presented comparable rejections (83-100%) to that of DuraMem™900 and lower ones compared to DuraMem™500, in spite of having a lower nominal cut-off of 400 Da. The disparities observed cannot be explained simply by the differences of ethanol permeability and initial cut-off of the membranes. In this case, the dead-end operation probably misrepresented the selectivity that could be expected. The ingredients in the neighborhood of the membrane carried by the high initial flux toward the membrane surface, probably blocked highly permeable outer membrane pores, causing a change in nominal MWCOs.

For the DuraMem™500 the rejections remained at high levels of 90-95%, without sensible losses in the permeate, but this was at the expense of lower permeate flux. The modification of the initial feed concentration resulted in a slight tendency to increase or decrease in rejection of solutes - the 2.5-fold increase in feed TSC reduced by approximately 5% the rejection of hypericins and up to 35% the permeate flux.

The DuraMem™200 showed the best efficiency for concentrating the extracts combined with sufficient fluxes and degree of recovery of permeability. The small amount of the permeating molecules was confirmed by the high rejection of total extract (~ 97%). Spectrophotometrically analyzed hypericins consistently showed almost complete rejection (> 99%), though the HPLC/MS detected some traces in the permeate, advisable for the lack of high sensitivity of a spectrophotometer at low-level concentrations (data not shown). Still it is interesting to note that some other valuable compounds were detected, as gamma-aminobutyric acid (GABA, 103.12 $gmol^{-1}$) that plays a role in regulating neuronal excitability in the brain.

Basically, the rejection towards the analyzed compounds decreased by decreasing the MWCOs of the membranes of the same type, and agreed with the size exclusion mechanism. However, despite the high rejection values, the concentration factor obtained for TPC and TFC was lower than the VRF used. This behavior may have been observed due to the establishment of fouling.

Modeling of permeate flux decline

Membrane fouling was characterized by the permeation curves, i.e. cumulative permeate volume per membrane area *versus* time V/A=f(t) in order to discriminate low-fouling conditions (slow-rate reduction) where the intrinsic membrane resistance is predominant and there are strong-fouling conditions with additional resistance to the filtration. The experimental data were fitted using the selected models (Table 2) and examples of curve-fits with the parameters identified after non-linear regression are presented in Figs. 2 and 3.

To address the impact of the membrane structure and properties, the flux decline through the membranes StarMem™240 and DuraMem™500 was compared during the treatment of extract E3 (Fig. 2). While the soluble solids increased from 1 to about 2 g L^{-1}, the fluxes decreased by 70% at very different rates. The experiments were carried out at the same TPM (20 bar) and not at the same initial flux. For the StarMem™240 (starting with high $J_{s,in}$ of 30 $Lm^{-2}h^{-1}$) the flux decreased very fast (0.6 h) while for the DuraMem™500 the flux gradually decreased, comparable reduction of the $J_{s,in}$ (11 L $m^{-2}h^{-1}$) was obtained after 6 hours of operation.

The analysis of Fig. 2 indicates that the combined pore blocking/cake formation model, having 3 fitting parameters (J_0, K_b, K_c) instead of 2 (J_0, K) for the classic models, had the best fits ($R^2 > 0.95$) to the non-linear increase of V/A for both membranes over the entire permeation run. There is a time interval in which the three kinetic models describing the surface fouling (complete, intermediate blocking and cake layer) also provided good data fits; the gap widens for longer durations.

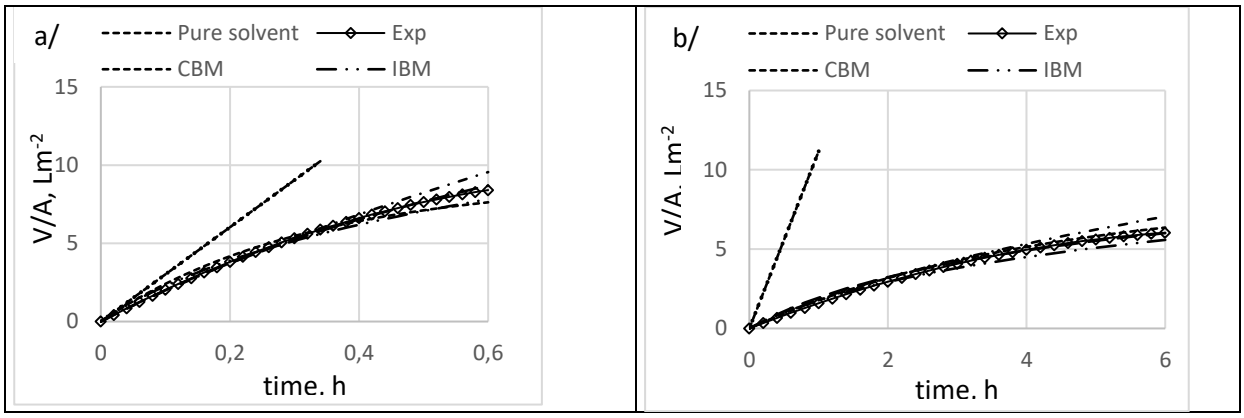

Figure 2. Experimental and calculated evolution of permeate volume *vs* time for the StarMem™240 (a) and DuraMem™500 (b) membranes in the presence of strong flux decline (extract E3; 20 bar)

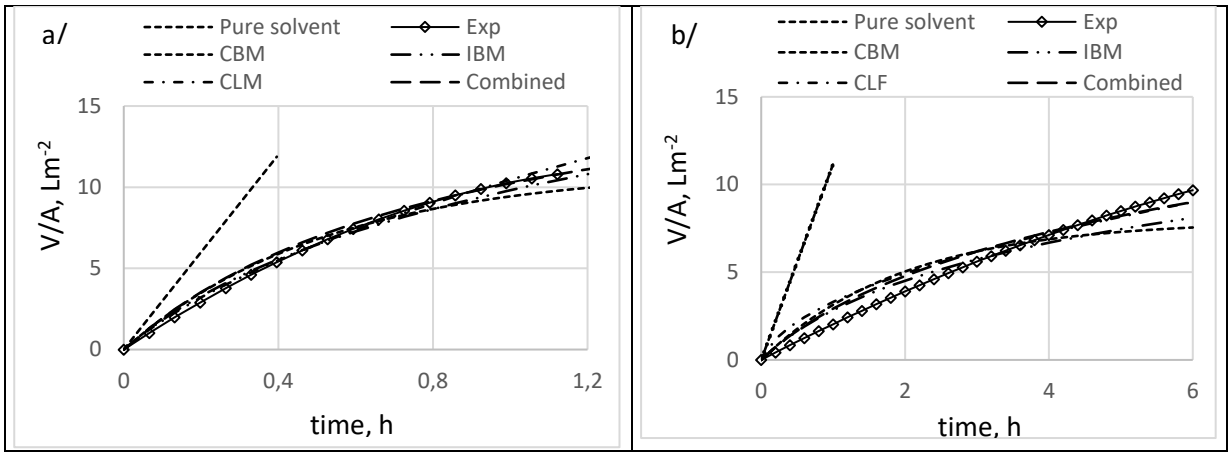

Figure 3. Fouling analysis for the StarMem™240 (a) and DuraMem™500 (b) membranes in the presence of slow flux decline (extract E1; 20 bar)

Given the polydispersity in solute size distribution and pore sizes of the membrane, at this early stage several pore-blocking mechanisms may take place simultaneously, producing a synergistic effect, followed by a transition to the cake layer at the latter stages [8, 10].

The higher values for the kinetic coefficients identified for the StarMem™240 compared to the DuraMem™500 specify a greater fouling tendency. The hydrophobic Starmem™240, not cross-linked, characterized by a small difference between the HSP values (Table 1 and 3) for ethanol and for polymer ($\Delta\delta_{HSP} \approx 3.3$ MPa$^{1/2}$), would have higher degree of swelling and behave elastically under pressure [5]. Consequently, the pore size enlargement may cause an increase in the initial fluxes and a negative effect on the rejection, as observed in the present study (Table 4). On the other side, the higher rejection and lower flux of DuraMem™500 can be attributed to its cross-linking rather to its slightly higher hydrophilicity, giving them a superior stability when exposed to ethanol solution.

The combined effects of the three hypothesized mechanisms: solute adsorption, hindered back diffusion, and increased resistance of the fouling layer can explain not only the increase of the total resistance to the permeation but also the variation in the separation efficiency. According to *Cassano et al.*, polyphenols have been shown to be the predominant cause of adsorptive fouling in the initial stage owing to the ability to form larger aggregates or complexes with other ingredients [13]. Consequently, the back-diffusion of smaller solutes is hindered and they can be also retained forming a variable cake layer. In this study, this was confirmed by analysis of the washing solvent after desorption of the fouled surface; phenolic compounds were predominant in the fouling layer, followed by hypericins and flavonoids, respectively, 22% TPC, 18% THC, and 10% TFC of the feed extract.

According to the results obtained, the process operating at lower TSC or VRF was less liable to be fouled. Fig. 3 shows the analysis during treatment of the extract E1 where the contents of TFC and TSC are by nearly 70% lower than in E3.].

For both membranes, there was again a quite rapid flux reduction at the beginning of the operation. A slow-rate reduction in the first 1.2 h was

observed for the StarMem^{TM}240 while no obvious flux decline was observed for the DuraMem^{TM}500 where the relation V/A=f(t) starts to deviate from linearity after 6 h. The low values obtained for the kinetic parameters incapable of satisfactory fits to the experimental data would reflect that there was a small development of the pore blocking and cake layer, the concentration by polarization was a major contributor to the observed flux decline. Apparently, in these favorable conditions, larger solutes tend to be swept away in the bulk volume rather than deposited; a loose reversible layer formed (concentration polarization) prevented initial pore blockage, so the transition to an irreversible packed structure (gel or deposit layer) could occur at the latter stages under severe concentration polarization.

At this point of the process, the main resistance can be reversible, so that the process had to be stopped for cleaning, before strong irreversible fouling happens. In fact, after the interruption of process and intermediate rinsing of the DuraMem^{TM}200 membrane, it was possible to further concentrate the E1 extracts and to reach contents for minor compounds hypericins comparable to that in the 3 steps sequential extraction. The dry solids content in the permeate was sufficiently low to permit direct reuse as extracting agent or washing solvent.

CONCLUSION

Among the membranes tested, all of them showed equally good high rejection towards hypericins, but the natural ratio hypericins: polyphenols: flavanoids is important for the biological susceptibility (of humans, bacteria and other plants), so the membrane with the highest rejection DuraMem^{TM}200 is predominantly preferred. Meanwhile the MWCO value does not play an important role, because the non-crosslinked StarMem^{TM}240 has much smaller rejections than the crosslinked DuraMem series even than the DuraMem^{TM}900 with the largest cut-off. DuraMem^{TM}200 membrane appeared to be suitable for the concentration of ethanolic extracts from *Hypericum perforatum*, but with relatively low permeance of 0.33 $Lm^{-2}bar^{-1}h^{-1}$, requiring frequent cleaning. Optimizing solid-liquid extraction by using emerging and more efficient techniques regarding extraction time, type and amount of solvent, and desorption kinetics, could help to reduce the flux decline and to make the combination of extraction and membrane processing more competitive.

REFERENCES

1. V. M. de Moraes, R. Rabelo, A. de L. Pereira, M. Hubinger, *Clean. Prod.*, **174** (2018).
2. R. Castro-Muñoz, V. l Fíla, *Trends Food Sci. Technol.*, **82**, 8 (2018).
3. A. Cassano, C. Conidi, R. Ruby-Figueroa, R. Castro-Muñoz, *Int. J. Mol. Sci*., **351**, 19 (2018).
4. B. Tylkowski, I. Tsibranska, *Physical Sciences Reviews*, **2** (2017).
5. A. Bocking, V. Koleva, J. Wind, Y. Thiermeyer, S. Blumenschein, R. Goebel, M. Skiborowski, M. Wessling, *J. Membr. Sci*., **217**, 575 (2019).
6. DuraMem Membrane Flat Sheet - Instructions for use, Evonik Industries, 2011.
7. J. Hermia, *Chem. Eng. Trans.*, **60**, 83 (1982).
8. G. Arend, S. Castoldi, M. Rezzadori, *BJFT*, **1**, 22 (2019).
9. G. Bolton; D. LaCasse, R. Kuriyel, *J. Membr. Sci.*, **277**, 75 (2006).
10. N. Amin, A. Mohammad, *J. Applied Membr. Science & Technology*, **22**, 85 (2018).
11. R. Zhang, Y. Ji, X. Zhang, E. J. Kennelly, C. Long, *J. Ethnopharmacol.*, **254** (2020).
12. M. Boykova, I. Saykova, I. Trayanov, *Scientific Works of UFT-Plovdiv*, **1**, 66 (2019).
13. A. Cassano, G. De Luca, C. Conidi, E. Drioli, *Coord. Chem. Rev.*, **35**, 45 (2017).